Constructing the Universe with Clusters of Galaxies, IAP 2000 meeting, Paris (France) July 2000
Florence Durret & Daniel Gerbal eds.

THE REDSHIFT SPACE POWER SPECTRUM OF REFLEX CLUSTERS OF GALAXIES

Peter Schuecker [(1)], Hans Böhringer [(1)], Luigi Guzzo [(2)], Chris A. Collins [(3)], Doris M. Neumann [(4)], Sabine Schindler [(3)], Wolfgang Voges [(1)], Sabrina De Grandi [(2)], Guido Chincarini [(2,5)], Ray Cruddace [(6)], Volker Müller [(7)], Thomas H. Reiprich [(1)], Jörg Retzlaff [(1)] and Peter Shaver [(8)]

[(1)] *Max-Planck-Institut für extraterrestrische Physik, Garching, Germany*
[(2)] *Osservatorio Astronomico di Brera, Merate, Italy*
[(3)] *Liverpool John Moores University, Liverpool, U.K.*
[(4)] *CEA Saclay, Service d'Astrophysique, Gif-sur-Yvette, France*
[(5)] *Dipartimento di Fisica, Universita degli Studi di Milano, Italy*
[(6)] *Naval Research Laboratory, Washington D.C., U.S.A.*
[(7)] *Astrophysikalisches Institut, Potsdam, Germany*
[(8)] *European Southern Observatory, Garching, Germany.*

The power spectrum is measured on scales from 15 to $800\,h^{-1}$ Mpc using the ROSAT-ESO Flux-Limited X-Ray (REFLEX) galaxy cluster catalogue. The REFLEX survey provides a sample of the 452 X-ray brightest southern clusters of galaxies with the nominal flux limit $S = 3.0 \times 10^{-12}\,\mathrm{erg\,s^{-1}\,cm^{-2}}$ for the ROSAT energy band $(0.1-2.4)\,\mathrm{keV}$. The most important result is the detection of a broad maximum within the comoving wavenumber range $0.022 \le k \le 0.030\,h\,\mathrm{Mpc}^{-1}$. A semi-analytic description of the biased nonlinear power spectrum in redshift space gives the best agreement for low-density Cold Dark Matter models with or without a cosmological constant. A more detailed description of the results will be presented in Astronomy & Astrophysics.

1 Introduction

The direct relation of the fluctuation power spectrum, $P(k)$, of the comoving density contrast, $\delta(\vec{r})$, to theoretical quantities makes it an ideal tool for the discrimination between different scenarios of cosmic structure formation and cosmological models in general. Power spectra obtained from optically selected cluster surveys (Peacock & West 1992; Einasto et al. 1993; Jing & Valdarnini 1993; Einasto et al. 1997; Retzlaff et al. 1998; Tadros, Efstathiou & Dalton 1998) are found to have slopes of about -1.8 for $k > 0.05\,h\,\mathrm{Mpc}^{-1}$ and a turnover or some indications for a turnover at $k \approx 0.03 - 0.05\,h\,\mathrm{Mpc}^{-1}$. Contrary to this, Miller & Batuski (2000) find no indication of a turnover in the distribution of Abell richness ≥ 1 clusters for $k \geq 0.009\,h\,\mathrm{Mpc}^{-1}$.[a] Measurements on scales $> 500\,h^{-1}\,\mathrm{Mpc}$ or $k < 0.013\,h\,\mathrm{Mpc}^{-1}$ where the cluster fluctuation signal is expected to be smaller than 1 percent are, however, extremely sensitive to errors in the sample selection. The resulting artificial fluctuations increase the measured power spectral densities and thus prevent any detection of a decreasing $P(k)$ on these large scales.

The current situation regarding the detection and the location of a turnover in the cluster power spectra appears to be very controversal with partially contradicting results. Physically, the scale of the expected turnover is closely linked to the horizon scale at matter-radiation equality. This introduces a specific scale into an otherwise almost scale-invariant primordial power spectrum and thus helps to discriminate between the different scenarios of cosmic structure formation discussed today. The narrow peak found for Abell/ACO clusters by Einasto et al. (1997) and Retzlaff et al. (1998) suggests a periodicity in the cluster distribution on scales of $120\,h^{-1}\,\mathrm{Mpc}$ and, if representative for the whole cluster population, is very difficult to reconcile with current structure formation models. The undoubted identification of the location and shape of this important spectral feature must, however, include a clear documentation of the quality of the sample from which it was derived.

Although the quality of optically selected large-area cluster samples has been improved during the past years by the introduction of, e.g., automatic cluster searches (e.g., Dalton et al. 1992, Lumsden et al. 1992, Collins et al. 1995) a major step towards precise fluctuation measurements on very large scales is offered by the use of X-ray selected cluster samples where also poor systems can be reliably identified and characterized within the global network of filaments or other large-scale structures.

This paper presents results of a power spectrum analysis obtained with a sample of 452 ROSAT ESO Flux-Limited (REFLEX) clusters of galaxies. A more detailed description is given in an article submitted to Astronomy & AStrophysics. A related study of the large-scale distribution of REFLEX clusters using the spatial two-point correlation function can be found in Collins et al. (2000).

2 The REFLEX cluster sample

The REFLEX clusters are detected in the ROSAT All-Sky Survey (Trümper 1993, Voges et al. 1999). They are distributed over an area of 4.24 sr (13 924 deg^2) in the southern hemisphere below +2.5 deg Declination. To reduce incompleteness caused by galactic obscuration and crowded stellar fields the sample excludes the area ± 20 deg around the galactic plane and 0.0987 sr at the Small and the Large Magellanic Clouds.

The sample is based on an MPE internal source catalogue extracted with a detection likelihood ≥ 7 from the ROSAT All-Sky Survey (RASS II). 54 076 southern sources have been re-analysed with the growth curve analysis method (Böhringer et al. 2000a,b, see also these proceedings) which is especially suited to the processing of extended sources. Although the data were analysed in all three ROSAT energy bands most weight is given to the hard band (0.5-2.0 keV) where 60 to 100 percent of the cluster emission is detected, the soft X-ray background is reduced by a factor of approximately 4, and the contamination through the majority of RASS II sources is lowest, so that the signal-to-noise for the detection of clusters is highest.

A complete identification of all cluster candidates and a measure of their redshifts has been performed in the framework of an ESO Key Programme (Böhringer et al. 1998, Guzzo et al. 1999). During this campaign, 431 X-ray targets were observed with an average of about 5 spectra per target. In Schuecker et al. (2000) detailed tests are described illustrating the

[a] The Hubble constant H_0 is given in units of $h = H_0/(100\,\mathrm{km\,s^{-1}\,Mpc^{-1}})$ and the X-ray source properties (luminosities, etc.) for $h = 0.5$, the cosmic density parameter is $\Omega_0 = 1$, and the normalized cosmological constant $\Omega_\Lambda = 0$.

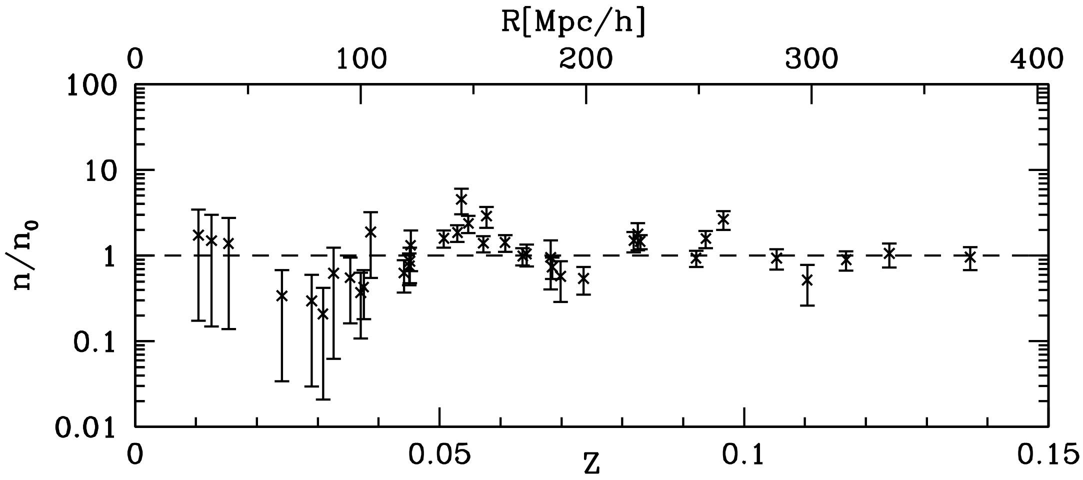

Figure 1: Normalized comoving cluster number densities as a function of redshift, z, and comoving radial distance, R. Vertical bars represent the formal 1σ Poisson errors. Note the quasi-periodic density fluctuations around an essentially constant mean.

high completeness of the REFLEX cluster sample. The test show that the data allow precise fluctuation measurements on scales up to about $800\,h^{-1}\,$Mpc.

As an example, Fig. 1 shows the normalized comoving number density computed along the redshift direction for comoving radial distances of $R \leq 400\,h^{-1}\,$Mpc correspond to $z \leq 0.15$. Maximum fluctuations of the order of 3 are found on small scales. They are successively smoothed out with increasing R. The quasi-periodic density variations have a wavelength of about $150\,h^{-1}\,$Mpc. No related feature is seen in the power spectrum at this scale (see below). The essentially constant mean comoving cluster density implies the absence of selection effects discriminating the more distant clusters. Note that the REFLEX survey covers the southern hemisphere so that a volume with a radius of $R = 400\,h^{-1}\,$Mpc gives a maximum comoving scale length of about $\lambda = 2R = 800\,h^{-1}\,$Mpc. However, comoving number densities remain constant up to $z = 0.3$, that is, on Giga parsec scales as will be shown in Böhringer et al. (in preparation).

3 Spectral analyses

For the determination of the power spectrum, two methods are compared. The first method uses the estimator (Schuecker et al. 1996a,b)

$$\hat{P}(k) \;=\; \frac{V}{\sum_{\vec{k}'}|W_{\vec{k}'}|^2}\,\left\langle\frac{|\hat{\delta}_{\vec{k}}|^2\;-\;\hat{D}}{1-|W_{\vec{k}}|^2}\right\rangle_{|\vec{k}|}\,, \tag{1}$$

where the fluctuation amplitudes are corrected for the effects of the survey window by

$$\hat{\delta}_{\vec{k}} \;=\; \frac{1}{\sum_i[\hat{\phi}(\vec{r}_i)]^{-1}}\,\sum_{i=1}^{N}[\hat{\phi}(\vec{r}_i)]^{-1}\,e^{i\vec{k}\cdot\vec{r}_i}\;-\;\frac{1}{\sum_j[\hat{\phi}(\vec{r}_j)]^{-1}}\,\sum_{j=1}^{M}[\hat{\phi}(\vec{r}_j)]^{-1}\,e^{i\vec{k}\cdot\vec{r}_j}\,. \tag{2}$$

The estimator of the discreteness noise is

$$\hat{D} \;=\; \frac{\sum_{i=1}^{N}(\hat{\phi}(\vec{r}_i))^{-2}}{\left[\sum_{i=1}^{N}(\hat{\phi}(\vec{r}_i))^{-1}\right]^2}\;+\;\frac{\sum_{j=1}^{M}(\hat{\phi}(\vec{r}_j))^{-2}}{\left[\sum_{j=1}^{M}(\hat{\phi}(\vec{r}_j))^{-1}\right]^2}\,. \tag{3}$$

The squared differences of the discrete Fourier transforms of the observed (inhomogeneous) and of the random distributions, both corrected for shot noise, are averaged over different directions and weighted by $(1 - |W_{\vec{k}}|^2)$ reducing the effects of the errors in the mean number density (Peacock & Nicholson 1991). The power spectral densities must be normalized by the volume V used to compute the Fourier transforms and by the total power of the Fourier transformed survey window. Whereas the number of observed objects N is fixed by the sample, the number of points used for the random sample M should be large enough so that their shot noise contributions can be subtracted with high accuracy. Both the observed and the random samples have the same position-dependent selection function, $\phi(\vec{r})$.

The second method to determine the power spectrum averages the fluctuation power over N_k modes per k shell (Feldman, Kaiser & Peacock 1994),

$$\hat{P}(k) = \frac{1}{N_k} \sum_{\vec{k}} |\hat{\mathcal{F}}(\vec{k})|^2 - \hat{\mathcal{D}}\,, \tag{4}$$

where the window-corrected Fourier-transformed density contrasts are given in a similar way as before,

$$\hat{\mathcal{F}}(\vec{k}) \; = \sum_{i=1}^{N} w(\vec{r}_i)\, e^{i\vec{k}\cdot\vec{r}_i} \; - \; \alpha \sum_{j=1}^{M} w(\vec{r}_j)\, e^{i\vec{k}\cdot\vec{r}_j}\,. \tag{5}$$

The total shot noise is estimated by

$$\hat{\mathcal{D}} \; = \; \alpha(1+\alpha) \sum_{j=1}^{M} w^2(\vec{r}_j)\, e^{-\vec{k}\cdot\vec{r}_j}\,, \tag{6}$$

where $\alpha = N/M$. For Gaussian fluctuations the weights $w(\vec{r}) = \frac{1}{1+n(\vec{r})P(k)}$ minimize the variance of the estimator, however, they require the *a priori* knowledge of $P(k)$, that is, the quantity one wants to measure, in addition to a fair estimate of the mean density, $n(\vec{r})$. Reasonable results are attainable if $n(\vec{r})$ is estimated by the observed luminosity function and the sensitivity map of the survey, and if $P(k)$ is approximated by a constant power spectrum, $P(k) = P_0 = \text{const}$.

The first test concerns the choice of the spectral estimator used for the analyses of the REFLEX data. We found that the differences between the power spectral densities obtained with eqs. (1) and (4) and the differences between the power spectra obtained with (4) for different P_0 are small compared to the errors introduced by the sample itself. We choose (1) for the spectral analyses because the exploration of the REFLEX data should start with a minimum of pre-assumptions about $P(k)$. Moreover, the REFLEX survey volume is comparatively symmetric so that in addition to the window correction term in eq. (1) no specific deconvolutions are performed. The remaining effects of the window functions are checked using the results obtained with N-body simulations (see Schuecker et al. 2000).

4 Observed power spectra

Many variants of cosmic structure formation models discussed today predict an almost linear slope of the power spectrum on scales $< 40\,h^{-1}\,$Mpc and a turnover into the primordial regime between 100 and $300\,h^{-1}\,$Mpc. To summarize our measurements in this interesting scale range, Fig. 2 shows the power spectral densities obtained with different *flux-limited* REFLEX subsamples. The volumes differ by a factor 19, enabling tests of possible volume-dependent effects. The superposed continuous and dashed lines in this and the following figures of this section are always the same. Their computation and interpretation is described below. In the following they may serve as a mere reference to compare the power spectra obtained with the different

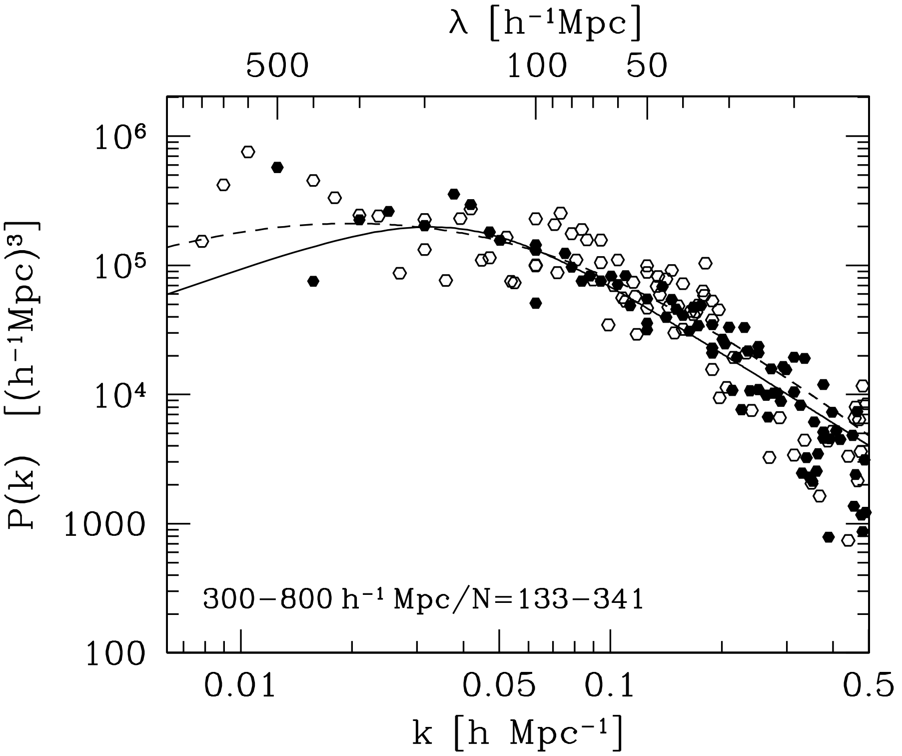

Figure 2: REFLEX power spectra of different flux-limited subsamples in volumes with box lengths between 300 and 800 h^{-1} Mpc (no corrections for differences in effective biasing). For reference, the spectral fits obtained with the phenomenological model (continuous line, see Peacock 1999, p. 530) and with the CDM-like model (dashed line) are superposed.

REFLEX subsamples. Fig. 3 compares the spectra obtained for two *volume-limited* subsamples with a spectrum obtained for a specific *flux-limited* subsample, all spectra are estimated within the same Fourier volume. Fig. 4 shows the combined power spectrum obtained with the best three subsamples which we regard as the basic result of the REFLEX power spectrum analyses. In the following a few more detailed remarks are given.

The point distribution in Fig. 2 outlines a corridor which can be devided into three parts. For $k > 0.1\,h\,\mathrm{Mpc}^{-1}$ the power spectral densities decrease approximately as k^{-2}. Between $0.02 \leq k \leq 0.1\,h\,\mathrm{Mpc}^{-1}$ the spectra bend into a flat distribution. The N-body simulations give 1σ standard deviations between 30 and 80 percent (including cosmic variance) in this scale range. For $k < 0.02\,h\,\mathrm{Mpc}^{-1}$ a second maximum is seen at $k \approx 0.01\,h\,\mathrm{Mpc}^{-1}$. We did not perform N-body simulations for such large scales. However, the delete-d jackknife resampling method (a variant of the boostrap method where the creation of artifical point pairs is avoided; see, e.g., Efron & Tibshirani 1993) gives 1σ error estimates of the order of 80 percent (cosmic variance not included). The detection of the second maximum in the power spectrum on such large scales, if real, would have very important implications on current structure formation models. However, as pointed out in the Introduction, measurements on such large scales are easily biased by very small systematic errors of the survey detection model. We postpone a detailed study of this very questionary feature to a subsequent paper. The present investigation concentrates more conservatively on the range $0.013 \leq k \leq 0.4\,h\,\mathrm{Mpc}^{-1}$ which is found to be free from *any* significant artifical fluctuations, which can be easily monitored by the available N-body simulations, and which contains density waves well sampled by the REFLEX clusters.

The spectra shown in Fig. 3 obtained with two *volume-limited* subsamples (upper and middle panel) show a broad maximum at $k \approx 0.03\,h\,\mathrm{Mpc}^{-1}$. A weak indication is found for a positive slope on larger scales. The second maximum of the power spectrum seen in Fig. 2 is not sampled

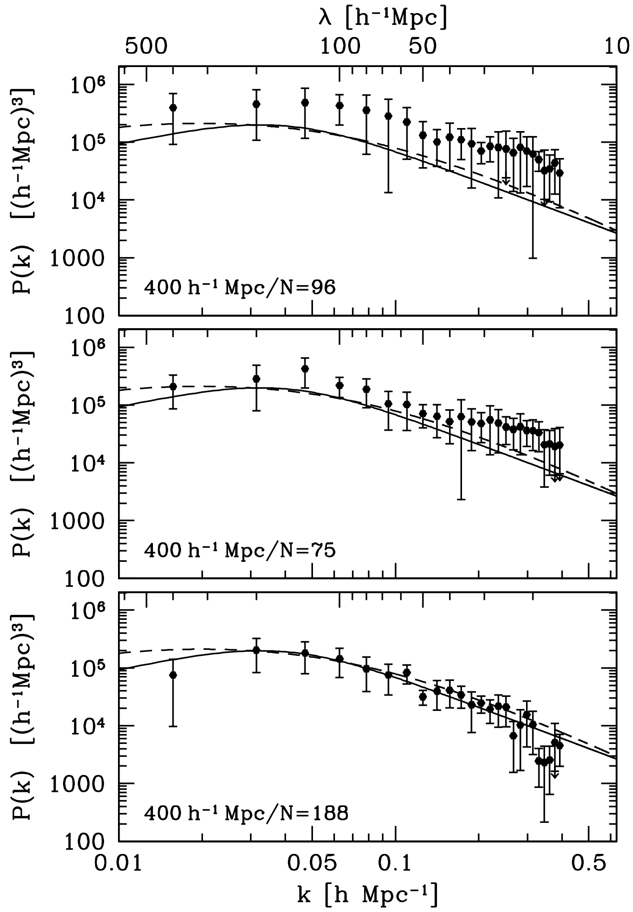

Figure 3: REFLEX power spectra of two volume-limited subsamples (upper two panel), and of one flux-limited (lower panel). The amplitudes of $P(k)$ increase with increasing lower luminosity limit as expected by standard biasing schemes.

because their sample volumes do not reach such large scales. The Fourier volumes are therefore restricted in both cases to $(400\,h\,\mathrm{Mpc}^{-1})^3$. For comparison the lower panel shows the power spectrum obtained with a *flux-limited* subsample estimated within the same volume as used for the volume-limited subsamples. In general, the overall shapes of the spectra obtained with the volume- and flux-limited subsamples are found to be similar, although minor differences might be seen on smaller scales. The three spectra also show that the amplitude increases with increasing lower X-ray luminosity of the subsample. However, larger sample sizes are needed to confirm the effect.

To summarize, basically all REFLEX spectra are consistent with a broad maximum of the cluster power spectrum at comoving wavenumbers around $k \approx 0.03\,h\,\mathrm{Mpc}^{-1}$ corresponding to wavelengths of about $200\,h^{-1}\,\mathrm{Mpc}$. A second maximum is found at $k = 0.01\,h^{-1}\,\mathrm{Mpc}$ corresponding to $600\,h^{-1}\,\mathrm{Mpc}$, but appears questionary. These findings are summarized in Fig. 4, showing the combined spectra obtained with three flux-limited subsamples. We regard this as a representative REFLEX power spectrum.

A standard SIMPLEX χ^2 minimization method is applied separately to the spectra obtained with the flux-limited subsamples to perform numerical fits from which the values of k_{max} and the shape parameter, Γ, of the linear power spectrum are deduced. This assumes that the power spectral densities of each individual spectrum are statistically independent. For the given REFLEX survey window ($|W_k|^2 \leq 0.082$ for all k and volumes studied), and for the given spacing of the k values of the measured $P(k)$ data at the multiples of the fundamental mode

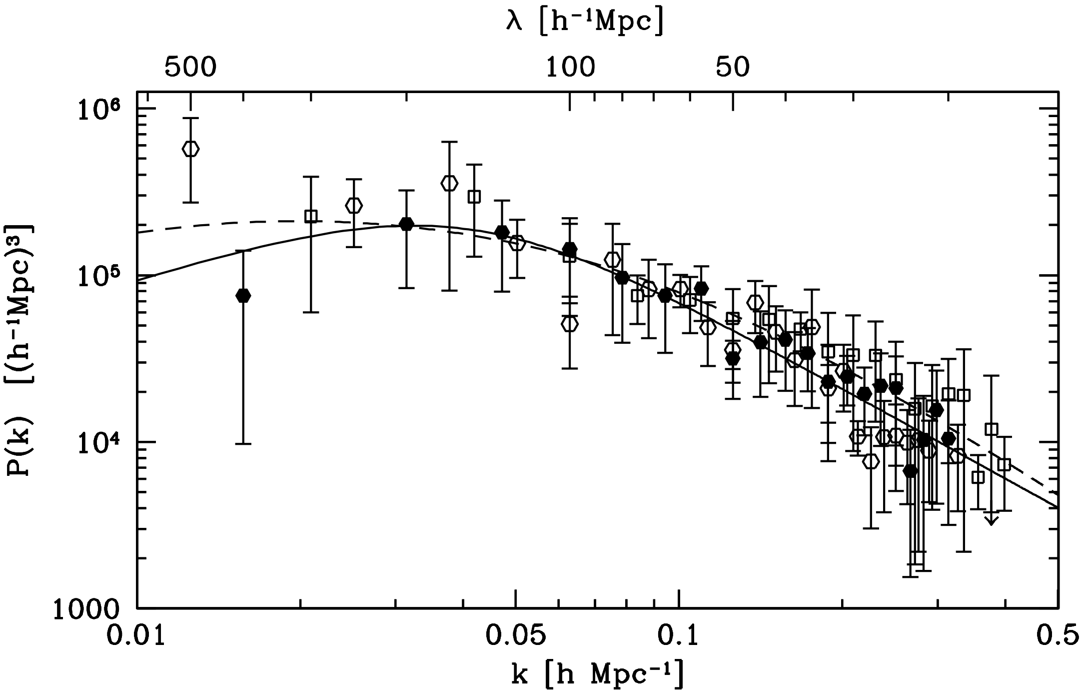

Figure 4: Combined REFLEX power spectrum obtained with three flux-limited subsamples, and their standard 1σ deviations adapted from N-body simulations. Not shown are the power spectral densities with wavenumbers $k \geq 0.4\,h\,\mathrm{Mpc}^{-1}$ because the corresponding density waves are only sparsely sampled by REFLEX. The continuous line is a fit of the phenomenological model (Peacock 1999, p. 530, the dashed line the CDM-like model fit using the flux-limited subsamples.

this is approximately the case. The values of $k_{\max}$ and Γ obtained from the fits are independent of the volumes used to perform the Fourier analyses strongly supporting the detection of a real maximum of $P(k)$ in the given k range. Averages and their formal 1σ standard deviations of $k_{\max}$ and Γ are

$$0.022 \pm 0.006 \leq k_{\max} \leq 0.030 \pm 0.005\,, \qquad \Gamma = 0.195 \pm 0.055\,. \tag{7}$$

Figure 5 compares the REFLEX power spectrum with the Abell/ACO (Retzlaff et al. 1998, see also Einasto et al. 1997) and the APM (Tadros et al. 1998) spectra. The respective amplitudes of the power spectra of the Abell/ACO and APM samples are 1.7 and 2.2 below REFLEX. This might be attributed to the different cluster luminosities contained in the samples. For $k \geq 0.08\,h\,\mathrm{Mpc}^{-1}$ the spectra give consistent slopes of approximately -1.8 although both the REFLEX and the Abell/ACO sample do not show the minimum at $k \approx 0.1\,h\,\mathrm{Mpc}^{-1}$ found with the APM sample. Regarding the maximum of $P(k)$ the Abell/ACO data suggest a comparatively narrow peak at $k_{\max} = 0.05\,h\,\mathrm{Mpc}^{-1}$ consistent with the estimate of Einasto et al. (1997). Contrary to this the REFLEX spectrum has a broad maximum which peaks in the range $0.022 \leq k_{\max} \leq 0.030\,h\,\mathrm{Mpc}^{-1}$. Note that the exact evaluation of the statistical significance of this difference is difficult to assess because the REFLEX and Abell/ACO power spectra are sampled in different ways. The broad maximum of the REFLEX spectrum appears to be more consistent with the APM sample if the REFLEX measurement at $500\,h^{-1}\,\mathrm{Mpc}$ is excluded.

Figure 6 compares the combined REFLEX power spectrum obtained with the three flux-limited subsamples with the spectrum obtained with a magnitude-limited sample of Durham/UKST galaxies (Hoyle et al. 1999). We chose this sample because of the comparatively large samples size (2501 galaxies, 1 in 3 sampling rate), the large volume (1 450 square degrees, $z \leq 0.1$), and the small effects of the survey window. Note that the upper continuous line is

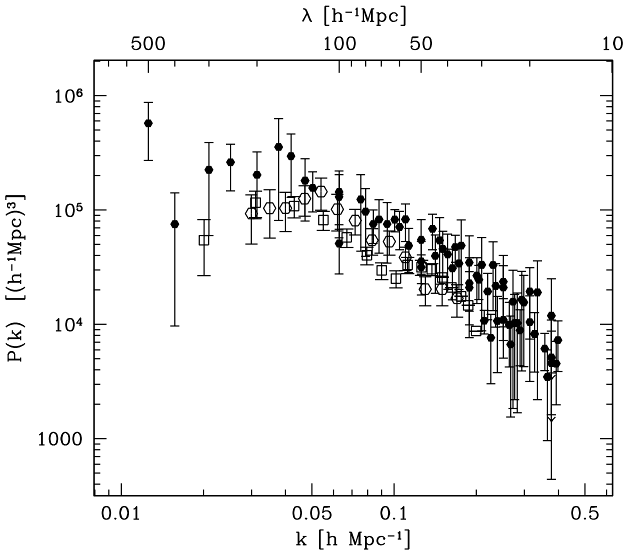

Figure 5: Combined REFLEX power spectrum obtained with the three subsamples (filled symbols) compared to the power spectrum obtained from Abell/ACO clusters (open hexagons) by Retzlaff et al. (1998) and from APM clusters (open squares) by Tadros et al. (1998).

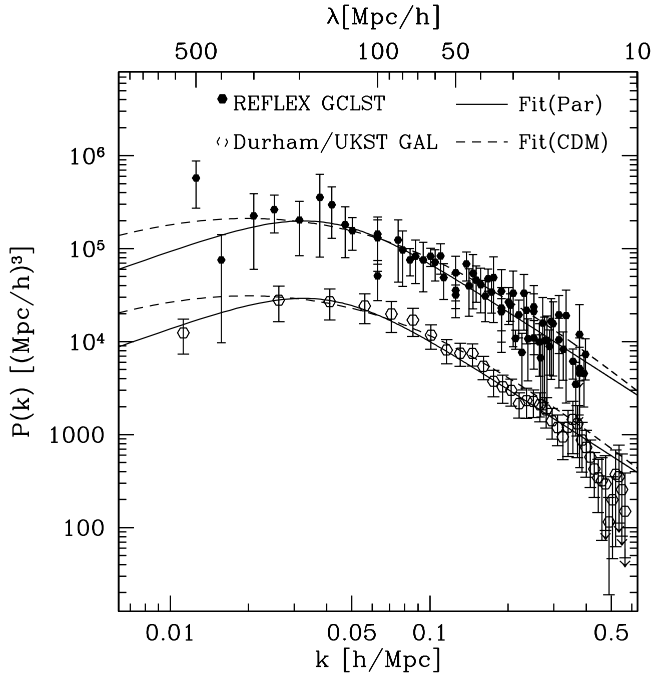

Figure 6: Combined power spectrum obtained with threee flux-limited REFLEX cluster subsamples (filled symbols, measurements on scales $< 20\,h^{-1}$ Mpc omitted) compared with the power spectrum of Durham/UKST galaxies (open symbols) obtained by Hoyle et al. (1999). The upper lines give the fit to the REFLEX cluster power spectra, the lower lines the same fits divided by the squared 'biasing factor' $b^2 = 2.6^2$. The continuous line is a fit of the phenomenological model (Par), the dashed line the CDM-like model fit (CDM) as described in Fig. 4.

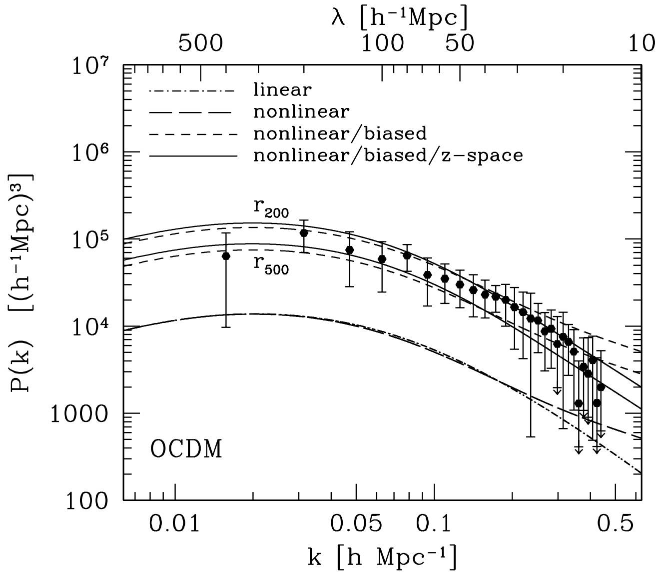

Figure 7: Test of the semi-analytic model with N-body simulations. Shown is the power spectrum averaged over 10 OCDM N-body simulations (filled symbols) of ideal clusters samples and their 1σ standard deviations (error bars). The lines represent the power spectra obtained with the semi-analytic model for the same model parameters as the N-body simulations ($\Omega_0 = 0.40$, $\Omega_\Lambda = 0$, $\Omega_b = 0.05$, $h = 0.60$, $\Gamma = 0.20$, $n = 1$, $\sigma_8 = 0.80$, i.e., cluster-normalized). Dashed-dotted line: linear matter power spectrum. Long-dashed line: evolved matter power spectrum. Short-dashed lines: evolved power spectrum including effective biasing. Continuous lines: last spectrum transformed into redshift space. The two types of spectra are shown for the empirical mass-luminosity relation obtained by Reiprich & Böhringer (1999) with r_{200} and r_{500}.

the fit of the phenomenological model (Peacock 1999, p. 530) to the REFLEX data, the upper dashed line the fit of a linear CDM-like model; the lower lines are the same fits shifted by the factor 6.8. For wavelengths $20 < \lambda < 300\,h^{-1}$ Mpc the overall shapes of the cluster and galaxy power spectra are very similar. The ratio of the linear biasing factors for the given REFLEX cluster subsample and the galaxy sample as deduced from the shift factor is $b = 2.6$.

5 Comparison with CDM models

To make a first comparison with cosmological models and an attempt to differentiate between their presently discussed variants, an outline of a semi-analytic model is given in Schuecker et al. (2000) for biased nonlinear power spectra in redshift space for clusters of galaxies. The model gives a good overview of the effects of different model parameters and is used to narrow the parameter ranges needed for a more detailed comparison with N-body simulations. Notice that a significant number of N-body simulations has to be performed for each parameter set in order to derive statistical meaningful error estimates which is planed for the second paper on the REFLEX power spectrum. The model spectra are computed with parameter values taken from the literature and are compared with the REFLEX power spectra. No evolution of structures is assumed within the redshift range covered by the REFLEX subsamples analyzed ($z < 0.15$, for an exact treatment see also Magira et al. 2000).

The semi-analytic model is tested against the 10 N-body simulations (OCDM) of ideal cluster samples. In Fig. 7 the lines give the theoretical spectra obtained under the different model assumptions, the filled symbols the average power spectral densities obtained from the N-body simulations, and the error bars their 1σ standard deviations. The overall agreement between model and simulation is good enough to separate between different scenarios of cosmic structure

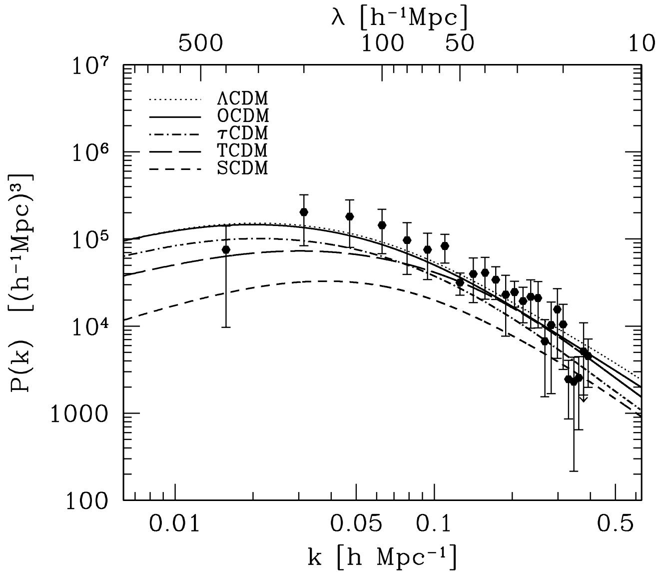

Figure 8: Comparison of observed power spectral densities and expectations of variants of CDM semi-analytic models for a flux-limited subsample.

formation. The largest ambiguity is introduced by the specific choice of the empirical mass-luminosity relation determined by Reiprich & Böhringer (1999). In the following the theoretical spectra obtained with r_{200} are shown because the corresponding cluster masses are expected to give better estimates of the virial masses.

As an example, in Fig. 8 the REFLEX power spectrum obtained with a flux-limited subsample is compared with different variants of CDM models. The standard Cold Dark Matter (SCDM) model with the COBE normalization as given in Bennett et al. (1994) is shown for reference. The open CDM (OCDM) model is cluster-normalized (combination of Eke, Cole & Frenk 1996, and Viana & Liddle 1996). For the low-density flat (ΛCDM) model see Liddle et al. (1996a,b). The tilted (TCDM) model is described in Moscardini et al. (2000) and the references given therein. The τCDM model is cluster-normalized according to Viana & Liddle (1996). The measured power spectra discriminate between the models, SCDM and TCDM are excluded, τCDM fits marginal the lower 1σ range, the open and ΛCDM models slightly underpredict the fluctuation amplitude but within the 1σ significance range.

To test the biasing trends we changed the ΛCDM normalization from $\sigma_8 = 0.93$ to $\sigma_8 = 0.70$ (similarly we could also change $\sigma_8 = 0.80$ to $\sigma_8 = 0.60$ for the OCDM model) yielding an acceptable fit to the flux-limited REFLEX power spectrum (open symbols and continuous line in Fig. 9). The ΛCDM spectra are then computed for the same volume-limited subsamples as used for the determination of the empirical spectra. The increase of the amplitude with the increasing lower X-ray luminosity – although at the detection limit of REFLEX – is well reproduced by the model, but not the apparent flattening of the slope on scales $< 100\,h^{-1}\,$Mpc. However, the errors of the slope measurements as deduced from the simulations are quite large so that the apparent difference might not be statistically significant.

6 Discussion and conclusions

The most important result of the present investigation is the detection of a broad maximum of the power spectrum of the fluctuations of comoving number density of X-ray selected cluster galaxies in the range $0.022 \le k \le 0.030\,h\,\mathrm{Mpc}^{-1}$ (Fig. 4). The maximum is flatter and peaks at a smaller wavenumber compared to optically selected cluster samples. On scales $0.02 \le k \le 0.4\,h\,\mathrm{Mpc}^{-1}$ the similiarity to the spectra obtained from optically selected galaxy samples is striking (Fig. 6).

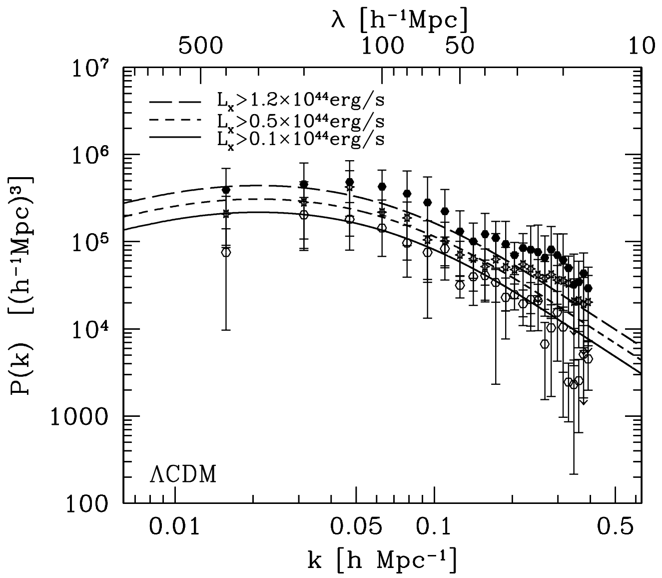

Figure 9: Comparison of observed power spectral densities and predictions of the ΛCDM semi-analytic model for a flux-limited subsample (open hexagons) and for the volume-limited subsamples: stars for $L_X > 0.5 \times 10^{44}\,\mathrm{erg\,s^{-1}}$ (subsample L050), filled symbols for $L_X > 1.2 \times 10^{44}\,\mathrm{erg\,s^{-1}}$ (subsample L120), $h = 0.5$. The Λ model is renormalized to $\sigma_8 = 0.70$ to give a good fit to the flux-limited subsample.

In this range the REFLEX data rule out galaxy formation models with strongly nonlinear biasing schemes.

The REFLEX data show extra fluctuation power on scales $k \approx 0.01\,h\,\mathrm{Mpc}^{-1}$ (Fig. 2). From our simulations we found that artifical power spectral densities of an order of magnitude can be easily produced on $500\,h^{-1}\,\mathrm{Mpc}$ scales if, e.g., the lower X-ray luminosity limit of $L_X^{\mathrm{min}} = 1.0 \times 10^{43}\,\mathrm{erg\,s^{-1}}$, which is used in the present investigation to get almost complete REFLEX subsamples, would be errorsly underestimated by a factor of about 1.5. Similarily, already on scales of $400\,h^{-1}\,\mathrm{Mpc}$ small changes in the method to estimate the radial part of the selection function change the power spectral densities by a factor 1.6. These two examples illustrate the difficulty to measure fluctuations on scales $> 400\,h^{-1}\,\mathrm{Mpc}$ and is the basic motivation to restrict the present investigations more conservatively to the small wavelength range.

Extra fluctuation power on $800\,h^{-1}\,\mathrm{Mpc}$ scales is also found for the Abell/ACO richness ≥ 1 clusters by Miller & Batuski (2000). In addition to the fact that they oversample the cluster power spectrum which mimic a more significant effect than the data can provide, it is difficult to understand how gradients in comoving cluster number density by a factor of 2, corrected with crude step-like radial selection functions, and the neglection of any corrections for galactic extinction can lead to precise fluctuation measurements at $800\,h^{-1}\,\mathrm{Mpc}$. It is surely insufficient to use cluster quadrant counts showing a scatter of 16 percent to justify fluctuation measurements aiming to detect fluctuations below the 1 percent level.

The REFLEX power spectra do not show any indication for a narrow peak at $k = 0.05\,h\,\mathrm{Mpc}^{-1}$. The report of such a feature in the power spectrum of Abell/ACO clusters and the interpretation as evidence for a regular distribution of galaxy clusters with a periodicity of $120\,h^{-1}\,\mathrm{Mpc}$ by Einasto et al. (1997) implies substantial difficulties for current models of structure formation. Retzlaff et al. (1998) who have found a similar but less peaked feature in the Abell/ACO cluster $P(k)$ used a large set of N-body simulations to demonstrate the potential importance of cosmic variance in this context. The discrepancy between REFLEX and Abell/ACO cluster results might be attributed to the additional 35 percent non-Abell/ACO/Supplement clusters included in the REFLEX catalogue. Unfortunately, the subtle selection effects imposed by optical cluster selection makes a quantitative discussion of this point almost impossible. In any case, due to current sample depths, cluster power spectrum analyses are restricted in general to volumes $< (500\,h^{-1}\,\mathrm{Mpc})^3$, and this imposes a spectral resolution $\Delta k = 0.013$ (fundamental mode) at best. Therefore, a significant detection of a feature such as a peak of width $\Delta k \approx 0.02$ is arguable at all.

The REFLEX spectra are compared with semi-analytic models describing the biased nonlinear power spectrum in redshift space. Most of the equations applied are calibrated with N-body simulations. We found that structure formation models with a low cosmic mass density (OCDM, ΛCDM) give the best representation of the REFLEX data (Fig. 8). Although the models could reproduce the observed changes of the amplitudes with samples of different luminosities, we regard the results are tendatively. Larger sample sizes are necessary to confirm this finding.

Acknowledgments

We thank Joachim Trümper and the ROSAT team for providing the RASS data fields and the EXSAS software, Harvey MacGillivray for providing the COSMOS galaxy catalogue, Rudolf Dümmler, Harald Ebeling, Alastair Edge, Andrew Fabian, Herbert Gursky, Silvano Molendi, Marguerite Pierre, Giampaolo Vettolani, Waltraut Seitter, and Gianni Zamorani for their help in the optical follow-up observations at ESO and for their work in the early phase of the project, Kathy Romer for providing some unpublished redshifts, Sabino Matarrese for some interesting discussions, and Stefano Borgani for critical reading of the manuscript. P.S. acknowledges the support by the Verbundforschung under the grant No. 50 OR 9708 35, H.B. the Verbundforschung under the grand No. 50 OR 93065.

References

1. Bennett, C. L., Kogut, A., Hinshaw, G., Banday, A. J., Wright, E. L., Gorski, K. M., Wilkinson, D. T., Weiss, R., Smoot, G. F., Meyer, S. S., Mather, J. C., Lubin, P., Loewenstein, K., Lineweaver, C., Keegstra, P., Kaita, E., Jackson, P. D., & Cheng, E. S., 1994, ApJ, 436, 423
2. Böhringer, H., Guzzo, L., Collins, C.A., Neumann, D.M., Schindler, S., Schuecker, P., Cruddace, R., De Grandi, S., Chincarini, G., Edge, A.C., MacGillivray, H.T., Shaver, P., Vettolani, G., & Voges, W., 1998, The Messenger, 94, 21
3. Böhringer, H., Schuecker, P., Guzzo, L., Collins, C.A., Voges, A., Schindler, S., Neumann, D.M., Chincarini, G., Cruddace, R.G., De Grandi, S., Edge, A.C., MacGillivray, H.T. & P. Shaver, 2000a, A&A (submitted)
4. Böhringer, H., Voges, W., Huchra, J.P., McLean, B., Giaconni, R.C., Burg, R., Mader, J., Schuecker, P., Simic, D., Komossa, S., Reiprich, T.H., Retzlaff, J., & Trümper, J., 2000b, ApJS, 129, 435
5. Collins, C.A., Guzzo, L., Nichol, R.C., & Lumsden, S.L., 1995, MNRAS, 274, 1071
6. Collins, C.A., Guzzo, L., Böhringer, H., Schuecker, P., Chincarini, G., Cruddace, R., De Grandi, S., Neumann, D.M., Schindler, S., & Voges, W., 2000, MNRAS (accepted)
7. Dalton, G.B., Efstathiou, G., Maddox, S.J., & Sutherland, W.J., 1992, ApJ, 390, L1
8. Efron, B., & Tibshirani, R.J., 1993, An Introduction to the Boostrap, Chapman & Hall, New York
9. Einasto, J., Gramann, M., Saar, E., & Targo, E., 1993, MNRAS, 260, 705
10. Einasto, J., Einasto, M., Gottlöber, S., Müller, V., Saar, E., Starobinsky, A.A., Tago, E., Tucker, D., Andernach, H., & Fritsch, P., 1997, Nature, 385, 139
11. Eke, V.R., Cole, S., & Frenk, C.S., 1996, MNRAS, 282, 263
12. Feldman, H.A., Kaiser, N., & Peacock, J.A., 1994, ApJ, 426, 23

13. Guzzo, L., Böhringer, H., Schuecker, P., Collins, C.A., Schindler, S., Neumann, D.M., De Grandi, S., Cruddace, R., Chincarini, G., Edge, A.C., Shaver, P.A., & Voges, W., 1999, The Messenger, 95, 27
14. Hoyle, F., Baugh, C.M., Shanks, T., & Ratcliffe, A., 1999, preprint astro-ph/9812137
15. Jing, Y.P., & Valdarnini, R., 1993, ApJ, 406, 6
16. Liddle, A.R., Lyth, D.H., Roberts, D., & Viana, P.T.P., 1996a, MNRAS, 278, 644
17. Liddle, A.R., Lyth, D.H., Viana, P.T.P., & White, M., 1996, MNRAS, 282, 281
18. Lumsden, S.L., Nichol, R.C., Collins, C.A., & Guzzo, L., 1992, MNRAS, 258, 1
19. Magira, H., Jing, Y.P., & Suto, Y., 2000, ApJ, 528, 30
20. Miller, C.J., & Batuski, D.J., 2000, preprint astro-ph/0002295
21. Moscardini, L., Matarrese, S., Lucchin, F., & Rosati, P., 2000, MNRAS (accepted), preprint astro-ph/9909273
22. Peacock, J., 1999, Cosmological Physics, Cambridge Univ. Press, Cambridge
23. Peacock, J., & Nicholson, D., 1991, MNRAS, 253, 307
24. Peacock, J.A., & West, M., 1992, MNRAS, 259, 494
25. Reiprich, H.T., & Böhringer, H., 1999, AN, 320, 296
26. Retzlaff, J., Borgani, S., Gottlöber, S., Klypin, A., & Müller, V., 1998, New Astronomy, 3, 631
27. Schuecker, P., Böhringer, H., Guzzo, L., Collins, C.A., Neumann, D.M., Schindler, S., Voges, W., De Grandi, S., Chincarini, G., Cruddace, R., Mueller, V., Reiprich, T.H., Retzlaff, J., Shaver, P., 2000, A&A (submitted)
28. Schuecker, P., Ott, H.-A., & Seitter, W.C., 1996a, ApJ, 459, 467
29. Schuecker, P., Ott, H.-A., & Seitter, W.C., 1996b, ApJ, 472, 485
30. Tadros, H., Efstathiou, G., & Dalton, G., 1998, MNRAS, 296, 995
31. Trümper, J., 1993, Science, 260, 1769
32. Viana, R.T.P., & Liddle, A.R., 1996, MNRAS, 281, 323
33. Voges, W., Aschenbach, B., Boller, Th., Bräuniger, H., Briel, U., Burkert, W., Dennerl, K., Engelhauser, J., Gruber, R., Haberl, F., Hartner, G., Hasinger, G., Kürster, M., Pfeffermann, E., Pietsch, W., Predehl, P. Rosso, C., Schmitt, J.H.M.M., Trümper, J., & Zimmermann, H.U., 1999, A&A, 349, 389